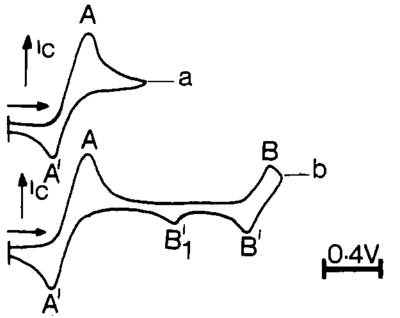

Figure 1. Voltammograms of $V^{IV}LCl_2$ at -30 °C (starting potential +0.8 V; sweep rate 0.2 $V{\cdot}s^{-1}$).

Scheme I

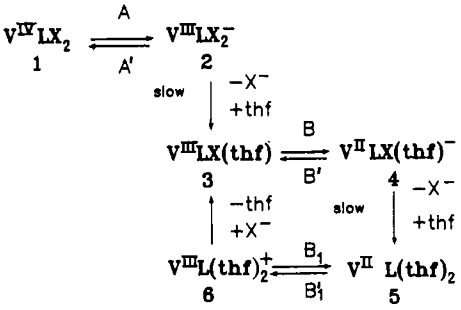

The vanadium(II) porphyrins $V^{II}L(PPhMe_2)_2$ and $V^{II}L(thf)_2$ (L = porphyrin macrocycle; thf = tetrahydrofuran) have been prepared recently[8,9] by chemical reduction of the dihalogenovanadium(IV) porphyrins $V^{IV}LX_2$ (X = Cl, Br); the V(III) complexes were not obtained. It has indeed been claimed, on the basis of theoretical studies,[10] that the V(II) should be more stable than the V(III) complexes.

We report in this note the electrosynthesis of the first V(III) porphyrin, $V^{III}LX(thf)$ (L = 5,10,15,20-tetra-*p*-tolylporphyrinate(2–); X = Cl), and of the V(II) complex $V^{II}L(thf)_2$ by reduction of $V^{IV}LX_2$.

In tetrahydrofuran[11] at -30 °C, on a platinum electrode, with 0.2 M tetrabutylammonium hexafluorophosphate as supporting electrolyte, the cyclic voltammogram of $V^{IV}LX_2$ shows two systems of reversible peaks A/A′ and B/B′ and an oxidation peak B'_1 (Figure 1).[12] When the sweep rate is decreased, the height of peak B increases relatively to that of A, and the height of peak B′ decreases relatively to that of B, whereas that of B'_1 increases; on a rotating disk electrode, wave B is not observed. These characteristics point to two successive reductions (A and B), both followed by a slow chemical reaction. Coulometries performed at respectively -0.8 and -1.1 V show that in each case one F is consumed. The results can thus be rationalized on the basis of Scheme I.

The V(III) complex $V^{III}LX(thf)$ (**3**) was isolated after an exhaustive controlled-potential electrolysis of **1**, evaporation of the solvent, and extraction by toluene. If mass spectrometric results are in favor of the $V^{III}LX$ formula (*m/e* 775 ($VLCl^+$), 720 (VL^+)), the molecular weight of complex **3** determined by cryoscopy in benzene was 1551, supporting a dimer formulation (M_r = 1510). Far-IR spectra in Nujol and in thf show the bands expected for vanadium–terminal chlorine stretching vibrations [ν(V–Cl) = 296 and 305 cm^{-1}, respectively], and the high-resolution ^1H NMR spectrum of **3** in C_6D_6 solution exhibits the resonance lines observed for diamagnetic porphyrin complexes. (Protons of *p*-Me-C_6H_4: δ 2.30 (s/12) (CH_3), 7.05 (m/8) (meta protons), 7.31 (m/8) (ortho protons). Protons of the pyrrolic rings: δ 8.46 (m/8).) All these data are consistent with a mononuclear formulation in a coordinating solvent (thf) and a dimeric arrangement in solvents like benzene or in the solid state. Compounds **2** and **3** cannot be formulated as π anions, the reduction potential of **1** being much too positive (+0.45 V; π anions are formed around -1.5 V[13]). The waves of the π anions do indeed appear in this region.[12]

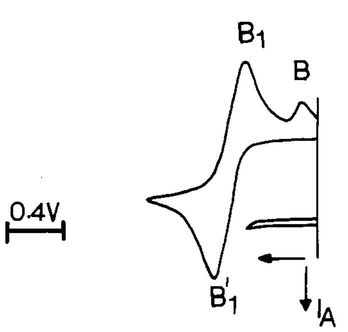

Figure 2. Voltammogram at -30 °C of $V^{II}L(thf)_2$ prepared electrochemically (starting potential -1V; sweep rate 0.1 $V{\cdot}s^{-1}$).

Controlled-potential reduction of $V^{III}LX(thf)$ at -1.1 V gives a solution whose UV spectrum is identical with that of $V^{II}L(thf)_2$ (**5**), which we have prepared chemically.[9] The cyclic voltammogram obtained after the electrolysis is identical with that of **5** (Figure 2). When the potential is scanned anodically starting from -1 V, peak B'_1 is observed (oxidation of **5** to **6**). On switching of the potential, peak B appears besides peak B_1, because of a partial transformation of **6** into **3** (see scheme); these features are typical of a square scheme with fast electrochemical reactions accompanied by a slow ligand exchange.[14]

Acknowledgment. We thank Dr. J. M. Barbe for his helpful assistance.

Registry No. **1**, 83582-04-1; **3**, 105694-21-1; **5**, 85961-79-1; tetrabutylammonium hexafluorophosphate, 3109-63-5.

---

[8] Poncet, J. L.; Barbe, J. M.; Guilard, R.; Oumous, H.; Lecomte, C.; Protas, J. *J. Chem. Soc., Chem. Commun.* **1982**, 1421.

[9] Oumous, H.; Lecomte, C.; Protas, J.; Poncet, J. L.; Barbe, J. M.; Guilard, R. *J. Chem. Soc., Dalton Trans.* **1984**, 2677.

[10] Zerner, M.; Gouterman, M. *Inorg. Chem.* **1966**, *5*, 1699.

[11] At room temperature, $V^{IV}LX_2$ is stable in neat THF but decomposes rapidly in the presence of $(TBA)PF_6$.

[12] The behavior of $V^{IV}LX_2$ is actually more complex. We describe here only the results that have a bearing on the preparation of the V^{III} complex. The complete results will be published in a further paper.

[13] Fuhrop, J. H.; Kadish, K. M.; Davis, D. G. *J. Am. Chem. Soc.* **1973**, *95*, 5140.

[14] Mugnier, Y.; Moise, C.; Laviron, E. *J. Organomet. Chem.* **1981**, *204*, 61. Laviron, E.; Roullier, L. *J. Electroanal. Chem.* **1985**, *186*, 1.

Contribution from the Department of Chemistry,
University of Colorado at Colorado Springs,
Colorado Springs, Colorado 80933-7150

Synthesis and Characterization of Molybdenum Tetracarbonyl Bound to the Novel Bridging Ligand 2,3-Bis(2-pyridyl)pyrazine

Ronald R. Ruminski* and Joyce O. Johnson

Received July 3, 1986

Recent investigations have explored the use of 2,3-bis(2-pyridyl)pyrazine (dpp) as a stable bidentate ligand in the preparations of mono and bimetallic ruthenium(II) polyazine complexes.[1,2] Those studies reported the visible absorption spectra and electrochemical characteristics that make $Ru(L)_3^{2+}$ (L = nitrogen aromatic heterocycle) systems a focus of study in ex-

---

[1] Braunstein, C. H.; Baker, A. D.; Strekas, T. C.; Gafney, H. D. *Inorg. Chem.* **1984**, *23*, 857.

[2] Brewer, K. J.; Murphy, R. W., Jr.; Spurlin, S. R.; Petersen, J. D. *Inorg. Chem.* **1986**, *25*, 883

cited-state electron-transfer and energy-transfer reactions for the absorption, storage, and use of visible solar energy.

Mono- and bimetallic tetracarbonyl centers bound to (through) bpym have been shown to be highly absorbing in the visible region of the spectrum and, due to the lower energy of the MLCT vs. LF bands, marginally photoreactive,[3,4] making them ideal antenna fragments for photon absorption and energy transfer.

Our research is directed toward the preparation and study of complexes that serve either as highly communicative electron transfer molecular frameworks,[5-8] or to directly absorb and transfer energy.[9,10] We now report the syntheses, electronic absorption and infrared spectra, electrochemistry, ^{13}C NMR spectra, and visible photochemistry of $[Mo(CO)_4]_{1,2}$dpp complexes.

Experimental Section

Materials. $Mo(CO)_6$, 2,3-bis(2-pyridyl)pyrazine (dpp), and the deuterated solvent used for ^{13}C NMR were obtained from Aldrich Chemicals. Other solvents were obtained from Fisher and used without redistillation. Elemental analyses were performed by Atlantic Microlab, Atlanta, GA.

Instrumentation. Electronic absorption spectra were recorded on a Beckman Model 5240 spectrophotometer with matching quartz cells.

Cyclic voltammograms were recorded on a Bio Analytic Systems CV-1B cyclic voltammograph with a Hewlett-Packard 7044A XY recorder. All potentials are reported vs. Ag/AgCl and are uncorrected for junction potentials.

Proton-decoupled ^{13}C NMR spectra were obtained on a Bruker Model WM-250 Fourier transform NMR spectrometer operating at 62.9 MHz. Samples were run in a 10.0-mm probe with 30% deuterated dichloromethane as an internal lock and reference ($\delta = 53.8$).

A continuous-beam photolysis apparatus previously described[8] was used for sample irradiations. Intensities of the apparatus were measured by Reinecke actinometry[11] at 546 and 577 nm. Solution preparation and measurement techniques are described elsewhere.[8]

Infrared spectra were recorded as solid KBr samples on a Nicolet Model 20DX FTIR instrument with a 1-cm^{-1} resolution.

Syntheses. The methods used for preparations of $[Mo(CO)_4]$dpp and $[Mo(CO)_4]_2$dpp are modifications of previously reported metal-tetracarbonyl complexes.[4,12]

$[Mo(CO)_4]$dpp. A mixture of 0.10 g (0.43 mmol) of dpp and 0.12 g (0.45 mmol) of $Mo(CO)_6$ in 25 mL of toluene was heated at reflux for 12 h under Ar in the dark. After the mixture was cooled to room temperature, petroleum ether was added and the product refrigerated overnight. The crude red product was collected by filtration on a sintered-glass filter funnel, washed with petroleum ether, and air-dried. The product was then dissolved on the funnel with $CHCl_3$ and suction filtered. The liquid was loaded on a 25 cm × 2 cm diameter silica gel (40–140 mesh) column that had been washed with $CHCl_3$. Red $[Mo(CO)_4]$dpp eluted slowly with $CHCl_3$. The liquid was collected, rotary evaporated to dryness, and stored under vacuum in the dark. Both the mono- and bimetallic complexes were formulated to contain a water of hydration, when it was later noted that drying beads in the toluene were saturated. Yield: 0.101 g (0.22 mmol), 51% Anal. Calcd. for $C_{18}H_{10}N_4O_4Mo{\cdot}H_2O$: C, 46.97; H, 2.63; N, 12.17. Found: C, 46.95; H, 2.50; N, 12.15.

$[Mo(CO)_4]_2$dpp. A mixture of 0.10 g (0.45 mmol) of dpp and 0.24 g (0.90 mmol) of $Mo(CO)_6$ in 25 mL of toluene was heated at reflux for 12 h under Ar in the dark. The product was precipitated, collected, and dried as described above. The product was dissolved with CH_2Cl_2 in the funnel and vacuum filtered. The liquid was loaded in fractions on a silica gel column (previously described) that had been washed with CH_2Cl_2. The blue $[Mo(CO)_4]_2$dpp fraction that separated from the red $[Mo(CO)_4]$dpp was collected and rotary evaporated to dryness in the dark. The product was then redissolved in CH_2Cl_2 and run down a freshly prepared silica column a second time. The product was collected, rotary evaporated to dryness in the dark, collected, and stored under vacuum in the dark. Yield: 0.206 g (0.31 mmol) 70% Anal. Calcd. for $C_{22}H_{10}N_4O_8Mo_2{\cdot}H_2O$: C, 39.56; H, 1.82; N, 8.39. Found: C, 38.77; H, 1.86; N, 8.27.

Table I. Electronic Absorption Data for $[M(CO)_4]$L Complexes

complex	solvent	λ_{max}, nm	$10^{-3}\epsilon$, M^{-1} cm^{-1}	assignt
$[Mo(CO)_4]$dpp[a]	$CHCl_3$	540	6.3	MLCT
		380 (sh)	4.2	$^1A_1,^1E_1 \leftarrow {}^1A_1$
	CH_2Cl_2	510	6.3	MLCT
		380 (sh)	4.3	$^1A_1,^1E_1 \leftarrow {}^1A_1$
		300	20	intraligand
	CH_3CN	480	5.3	MLCT
		380 (sh)	3.9	$^1A_1,^1E_1 \leftarrow {}^1A_1$
		300	21	intraligand
$[Mo(CO)_4]_2$dpp[a]	$CHCl_3$	630	12	MLCT
		375 (sh)	6.0	$^1A_1,^1E_1 \leftarrow {}^1A_1$
		325 (sh)	17	
		300	20	intraligand
	CH_2Cl_2	610	12	MLCT
		380 (sh)	6.0	$^1A_1,^1E_1 \leftarrow {}^1A_1$
		320 (sh)	19	
		300	22	intraligand
	CH_3CN	540	12	MLCT
		380 (sh)	5.5	$^1A_1,^1E_1 \leftarrow {}^1A_1$
		320 (sh)	19	
		300	24	intraligand
$[Mo(CO)_4]$bpym[b]	CH_2Cl_2	508		MLCT
		379		
$[Mo(CO)_4]_2$bpym[b]	CH_2Cl_2	675		MLCT
		440		

[a] This work; sh = shoulder. [b] Reference 3.

Table II. Infrared and Electrochemical[a] Data for $[Mo(CO)_4]_{1,2}$L Complexes

complex	infrared freq,[b] cm^{-1} CO	infrared freq,[b] cm^{-1} L	ref
$[Mo(CO)_4]$dpp	2016, 1914, 1882, 1819	1550, 1396	c
$[Mo(CO)_4]_2$dpp	2012, 1905, 1879, 1824	d, 1401	c
dpp		1583, 1390	
$[Mo(CO)_4]$bpym	2014, 1912, 1869, 1833	d, 1406	3
$[Mo(CO)_4]_2$bpym	2013, 1920, 1896, 1837	d, 1420	3
bpym		1560, 1400	3
$[Mo(CO)_4]$bpy	2014, 1920, 1882, 1830		12

[a] Oxidation potentials were measured by cyclic voltammetry in CH_2Cl_2, 0.1 M TBAP, at 100 mV/s vs. Ag/AgCl electrode. Potential of the oxidation wave: for $[Mo(CO)_4]$dpp, +0.905 V; for $[Mo(CO)_4]_2$dpp, +0.895 V. [b] Infrared samples recorded as solids in KBr. [c] This work. [d] Reportedly too broad to observe.

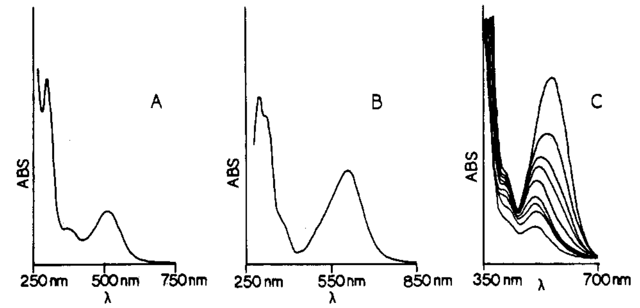

Figure 1. Visible-UV absorption spectra of (a) $[Mo(CO)_4]$dpp in CH_2Cl_2, (b) $[Mo(CO)_4]_2$dpp in CH_2Cl_2, and (c) $[Mo(CO)_4]_2$dpp in CH_3CN, indicating thermal decomposition to form the monometallic complex, followed by additional reaction.

Results and Discussion

The $[Mo(CO)_4]$dpp complex exhibits a solvent-dependent ($\epsilon > 1000\ M^{-1}\ cm^{-1}$) absorption in the visible region of the spectrum (Table I, Figure 1a). A solvent-dependent wavelength maximum has been previously noted when the absorption was due to a MLCT $L_{p_{\pi^*}} \leftarrow M_{d_\pi}$ transition.[3,4,13-15] Due to the large molar absorptivity,

---

(3) Overton, C.; Connor, J. A. *Polyhedron* **1982**, *1*, 53.
(4) Moore, K. J.; Petersen, J. D. *Polyhedron* **1983**, *2*, 279.
(5) Ruminski, R. R.; Petersen, J. D. *Inorg. Chim. Acta* **1984**, *88*, 63.
(6) Ruminski, R. R.; Petersen, J. D. *Inorg. Chim. Acta* **1985**, *97*, 129.
(7) Ruminski, R. R. *Inorg. Chim. Acta* **1985**, *103*, 159.
(8) Hiskey, M. A.; Ruminski, R. R. *Inorg. Chim. Acta* **1986**, *112*, 189.
(9) Ruminski, R. R.; Petersen, J. D. *Inorg. Chem.* **1982**, *21*, 3706.
(10) Ruminski, R. R.; Van Tassel, K. D.; Petersen, J. D. *Inorg. Chem.* **1985**, *23*, 4380.
(11) Wegner, E. E.; Adamson, A. *J. Am. Chem. Soc.* **1966**, *88*, 394.
(12) Stiddard, M. H. B. *J. Chem. Soc.* **1962**, 4712.
(13) Burgess, J. *J. Organomet. Chem.* **1969**, *19*, 218.
(14) Wrighton, M. S.; Morse, D. L. *J. Organomet. Chem.* **1975**, *97*, 405.
(15) Saito, H.; Fumita, J.; Saito, K. *Bull. Chem. Soc. Jpn.* **1968**, *41*, 863.

Table III. ^{13}C NMR Spectra of dpp and $[Mo(CO)_4]_{1,2}$dpp Complexes

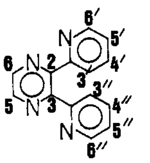

complex	δ(^{13}C)^a C(6),C(5)	C(6′),C(6″)	C(5′),C(5″)	C(4′),C(4″)	C(3′),C(3″)
dpp	148.85	142.96	123.30	136.71	124.33
$[Mo(CO)_4]_2$dpp	153.40	143.96	126.79	136.52	127.94
$[Mo(CO)_4]$dpp	152.65	144.59	*b*	138.02	127.17
	149.82	142.68	124.23	136.05	*b*

^{a}Chemical shift in CH_2Cl_2 reported vs. Me_4Si. ^{b}Signals at 125.30 ppm and 125.13 ppm not specifically assignable.

solvent dependence of the absorption, and similarity to spectra of previously reported $[Mo(CO)_4]$L complexes, we assign the lowest energy absorption of $[Mo(CO)_4]$dpp as MLCT $\text{dpp}_{p_{\pi^*}} \leftarrow \text{Mo}_{d_\pi}$.

The wavelength of the MLCT absorption of $[Mo(CO)_4]$L complexes in a common solvent has been interpreted as a reflection of the relative electron-withdrawing ability of the ligand.[3,4] The MLCT wavelengths of $[Mo(CO)_4]$bpym and $[Mo(CO)_4]$dpp are identical within experimental observation, which indicates an approximate parity of the electron-withdrawing ability of the bpym and dpp ligands upon the $[Mo(CO)_4]$ fragment. By analogy with other $[Mo(CO)_4]$L complexes, we assign the 380-nm absorption shoulder as being due to the $^1A_1,^1E_1 \leftarrow {}^1A_1$ LF transition.[3,4,14,16] The large molar absorptivity of the LF transition has previously been attributed as being due to some MLCT character in the transition. We assign the highest energy transition at 300 nm to a $\text{dpp}_{\pi^*} \leftarrow \pi$ intraligand transition.

The $[Mo(CO)_4]_2$dpp complex also exhibits a solvent-dependent ($\epsilon > 1000\ M^{-1}\ cm^{-1}$) absorption in the visible spectrum. By analogy to the equivalent monometallic complex, and $[Mo(CO)_4]_2$bpym,[3] we assign this as a MLCT $\text{dpp}_{p_{\pi^*}} \leftarrow \text{Mo}_{d_\pi}$ transition. The wavelength of the MLCT absorption for $[Mo(CO)_4]_2$dpp is 100 nm (in CH_2Cl_2) longer than for $[Mo(CO)_4]$dpp. This increase is similar to wavelength increases noted for the $[Mo(CO)_4]_{1,2}$bpym[3] and Ru(II) bpym-bridged systems.[9,17,18] This wavelength increase has been interpreted as being due to both (1) metal–metal interaction resulting in a higher energy bimetallic vs. monometallic d_π nonbonding HOMO and (2) a lower bimetallic bridging ligand p_{π^*} LUMO.[1,4,6,9] Metal–metal interaction through bpym was verified electrochemically by a 0.15–0.18 V more positive first oxidation potential of the bimetallic vs. the corresponding monometallic Ru(II) systems. In contrast to this, when dpp was the bridging ligand for Ru(II) bimetallic systems, the first oxidation potentials were equivalent for the mono- and bimetallic species. This was interpreted as indicating little metal–metal delocalization.

Cyclic voltammograms for $[Mo(CO)_4]$dpp and $[Mo(CO)_4]_2$dpp are electrochemically irreversible upon one-electron oxidations, with no return cathodic waves (Table II), and the potentials for one-electron oxidations of the mono- and bimetallic species are equal (within experimental error, 0.01 V). This may be interpreted as indicating little $[Mo(CO)_4]$–$[Mo(CO)_4]$ interaction through the dpp bridge, as in the Ru(II) complexes. Lowering of the MLCT absorption in $[Mo(CO)_4]_2$dpp may be primarily due to lowering of the dpp_{π^*} LUMO rather than strong metal–metal interaction.

A possible explanation for the limited metal–metal interaction may be the nonplanar configuration of the dpp bridging ligand because of 3′,3″-H,H steric interaction as has been demonstrated for Ru(II) systems.[1]

The $[Mo(CO)_4]_{1,2}$dpp complexes are both thermally reactive in deoxygenated room-temperature CH_3CN. The $[Mo(CO)_4]_2$dpp complex initially reacts to form the $[Mo(CO)_4]$dpp complex as evidenced by the gradual MLCT wavelength change from 540 nm for $[Mo(CO)_4]_2$dpp to 480 nm for $[Mo(CO)_4]$dpp (Figure 1c). This is then followed by a decrease in absorbance without wavelength change. The final products have not been identified, however, it is probable there is no Mo–dpp coordination owing to the lack of any visible absorption.

The infrared spectra of the $[Mo(CO)_4]_{1,2}$dpp complexes were recorded as a solid in KBr and reported in Table II. The spectra in the carbonyl region (2100–1800 cm^{-1}) reflect the four CO stretching frequencies expected for the $[Mo(CO)_4]$dpp moiety. The observed CO frequencies are typical mono- or bimetallic $Mo(CO)_4$ complexes.[3,11] Ring stretching modes reported in Table II are also characteristic for aromatic diimine rings.[19]

The $[Mo(CO)_4]_{1,2}$dpp complexes were irradiated in deoxygenated CH_2Cl_2 solutions 546 and 577 nm, respectively, into the MLCT bands. Extended irradiations show minimal ($\Phi_{max} < 0.0005$) reactant loss, which is typical for a low-spin d^6 system in which the MLCT state is the lowest lying excited state.[9,14,16,20-23]

^{13}C NMR spectra for dpp, $[Mo(CO)_4]$dpp, and $[Mo(CO)_4]_{1,2}$dpp were recorded in deuterated dichloromethane (Table III). The assignment of dpp ligand signals is based on those for bpy[3,4] and bpym ligands.[3,4,24] Assignment of signals for $[Mo(CO)_4]_2$dpp is relatively unambiguous, based on the dpp ligand. Assignment of C(6),C(5), C(6′),C(6″), and C(4′),C(4″) signals for $[Mo(CO)_4]$dpp is also direct, while the C(5′),C(5″) and C(3′),C(3″) signals are less certain. The effect of bimetallic coordination vs. dpp for C(5′) and C(3′) is a +3.5 ppm downfield shift, implying approximately equivalent electron-withdrawing effects on C(3′) and C(5′). On the basis of additivity of chemical shifts,[24] the resonance at 127.15 ppm is most likely due to C(3′) and the resonance at 124.38 ppm is due to C(5″). The signals at 125.20 and 125.13 ppm are from C(5′) and C(3″), although exact assignment is not possible. The previously reported downfield shift of all bridging ligand carbons in $M(CO)_4$ complexes[3,4] has been interpreted as resulting from competitive $M_{d_\pi} \rightarrow CO_{p_{\pi^*}}$ vs. $M_{d_\pi} \rightarrow$ bridging ligand p_{π^*} back-bonding.

We have recently prepared the $[Cr(CO)_4]$dpp and $[W(CO)_4]$dpp complexes and are currently working on the preparation and study of the homo- and heterobimetallic complexes.

Supplementary Material Available: Figures showing ^{13}C NMR and infrared spectra and cyclic voltammograms of the $[Mo(CO)_4]_{1,2}$ complexes (3 pages). Ordering information is given on any current masthead page.

---

(16) Wrighton, M. S.; Abrahamson, H. B. *Inorg. Chem.* **1978**, *17*, 3385.
(17) Dose, E. V.; Wilson, L. J. *Inorg. Chem.* **1978**, *17*, 2660.
(18) Hunziker, M.; Ludi, A. *J. Am. Chem. Soc.* **1977**, *99*, 7370.
(19) Basu, A.; Gafney, H. A.; Strekas, T. C. *Inorg. Chem.* **1981**, *21*, 2231.
(20) Malouf, G.; Ford, P. C. *J. Am. Chem. Soc.* **1977**, *99*, 7213.
(21) Malouf, G.; Ford, P. C. *J. Am. Chem. Soc.* **1974**, *96*, 601.
(22) Figard, J. A.; Petersen, J. D. *Inorg. Chem.* **1978**, *17*, 1059.
(23) Gelroth, J. A.; Figard, J. A.; Petersen, J. D. *J. Am. Chem. Soc.* **1979**, *101*, 3649.
(24) Ruminski, R. R.; Petersen, J. D. *Inorg. Chim. Acta* **1982**, *65*, L177.